SICCI (Sea Ice Climate Change Initiative) & SPICES (Space-borne observations for detecting and forecasting sea ice cover extremes)

Sea Ice Concentration (SIC) Round Robin Data Package (RRDP)

Doc Ref: RRDP-02-19

Version: 2.2

Date: February 07 2019

This page intentionslly left blank

Change Record

Issue	Date	Reason for Change	Author
1.0	26 November 2012	First Issue	Leif Toudal Pedersen, Roberto Saldo
1.2	15 August 2015	Revised issue for publication of SICCI1 SIC RRDP	Leif Toudal Pedersen, Natalia Ivanova, Stefan Kern, Roberto Saldo, Georg Heygster, Rasmus Tonboe, Marcus Huntemann
2.0	31 May 2017	Updated with more Antarctic data, ASCAT A+B data, SMOS data, SMAP data, QuikSCAT data contributed by SPICES EU project Various explanations improved	Leif Toudal Pedersen, Roberto Saldo, Natalia Ivanova, Stefan Kern, Fanny Ardhuin, Georg Heygster, Rasmus Tonboe, Marcus Huntemann, Lars Kaleschke, Burcu Ozsoy,
2.1	7 February 2019	Fixing two bugs in the accumulated variables from ERA Interim. The older version (before 2.2) should not be used for time series analysis using the accumulated ERA-Interim variables.	Leif Toudal Pedersen

Authorship

Role	Name	Signature
Written by:	Leif Toudal Pedersen, Roberto Saldo	ltp@space.dtu.dk
Checked by:	Stefan Kern, Rasmus Tonboe	
Authorised by:		

Distribution

Organisation	Names	Contact Details
ESA	Pascal Lecomte	Pascal.Lecomte@esa.int
NERSC	Stein Sandven, Natalia Ivanova	Stein.Sandven@nersc.no; Natalia.ivanova@nersc.no
Logica	Gary Timms,	gary.timms@logica.com;
Met.no	Thomas Lavergne, Atle Sørensen	t.lavergne@met.no; atlems@met.no
DMI	Rasmus Tonboe	rtt@dmi.dk
DTU	Roberto Saldo, René Forsberg, Henning Skriver, Henriette Skourup	rs@space.dtu.dk; rf@space.dtu.dk; hsk@space.dtu.dk
FMI	Marko Mäkynen, Eero Rinne, Jari Haapala	marko.makynen@fmi.fi; eero.rinne@fmi.fi;

Organisation	Names	Contact Details
University of Hamburg	Stefan Kern	stefan.kern@zmaw.de
University of Bremen	Georg Heygster	heygster@uni-bremen.de
MPI-M	Dirk Notz	dirk.notz@zmaw.de
Ifremer	Fanny Ardhuin	Fanny.Ardhuin@ifremer.fr

Table of Contents

List of Figures

No table of figures entries found.

List of Tables

1   Introduction

1.1   Purpose and Scope

This document describes the Round Robin datasets (RRDP) for the Sea Ice Concentration Essential Climate Variables products to be produced in ESA's Climate Change Initiative.

The RRDP is a set of comma separated ASCII files which contain reference sea ice concentrations and/or other relevant data and co-located satellite TBs extracted from the SMMR, SSMI and AMSR-E/AMSR2 swath datasets to be used to for ice concentration calculations.

The dataset should be easy to use by reading the files line by line, calculate SIC from the given TBs and compare with the given reference SIC.

1.2   Document Structure

The document includes the RRDP description for Sea Ice Concentration, including information about how the dataset was generated and the choices made.

1.3   Applicable Documents

The following table lists the Applicable Documents that have a direct impact on the contents of this document.

Acronym	Title	Reference	Issue
AD-1	Sea Ice ECV Project Management Plan	ESA-CCI_SICCI_PMP_D6.1_v1.1	1.1
AD-2	Sea Ice ECV Product Validation Plan	ESA-CCI_SICCI_PVP	
AD-3	Sea Ice ECV Data Access and Requirements Document	ESA-CCI_SICCI_DARD	
D1.2+D1.3 +D1.4	Reference datasets	SPICES H2020 deliverable	1.0

Table 1-1: Applicable Documents

1.4   Applicable Standards

Acronym	Title	Reference	Issue

Table 1-2: Applicable Standards

1.5   Acronyms and Abbreviations

Acronym	Meaning
ACDD	Attribute Convention for Dataset Discovery
AMSR-E	Advanced Microwave Scanning Radiometer aboard EOS
AMSR2	Advanced Microwave Scanning Radiometer version 2
AO	Announcement of Opportunity
ASAR	Advanced Synthetic Aperture Radar (on ENVISAT)
ASCAT	Advanced Scatterometer (on EUMETSAT MetOp series of satellites)
ASCII	American Standard Code for Information Interchange
ASIRAS	Airborne Synthetic Aperture and Interferometric Radar Altimeter System
ATBD	Algorithm Theoretical Basis Document
CF	Climate and Forecasting
CM-SAF	Climate Monitoring Satellite Application Facility
CRREL	Cold Regions Research and Engineering Lab
DMI	Danish Meteorological Institute
DMSP	Defence Meteorological Satellite Program
DTU	Technical University of Denmark
DWD	Deutscher Wetterdienst
EASE	Equal Area Scalable Earth-Grid
ECV	Essential Climate Variable
Envisat	Environmental Satellite
EO	Earth Observation
ERS	European Remote Sensing Satellite
ESA	European Space Agency
EUMETSAT	European Organisation for the Exploitation of Meteorological Satellites
FB	Freeboard
FCDR	Fundamental Climate Data Record
FOC	Free of Charge
FOV	Field-of-View
FTP	File Transfer Protocol
GB	GigaByte
GCOM	Global Change Observation Mission
GHRSST	Group for High Resolution Sea Surface Temperature
H	Horizontal polarization
H+V	Horizontal and vertical polarization
IDL	Interactive Data Language
ISF	Ice Surface Fraction
Matlab	Matrix Laboratory
MB	MegaByte
MIZ	Marginal ice zone
MODIS	Moderate Resolution Imaging Spectroradiometer
MPF	Melt Pond Fraction

Acronym	Meaning
n.a.	Not applicable
NERSC	Nansen Environmental and Remote Sensing Center
NetCDF	Network Common Data Format
NH	Northern hemisphere
NSIDC	National Snow and Ice Data Center
OIB	Operation Ice Bridge
OSI-SAF	Ocean and Sea Ice Satellite Application Facility
OWF	Open Water Fraction
PDGS	Payload Data Ground System
PI	Principal Investigator
PMR	Passive Microwave Radiometry
PMW	Passive Microwave
PRF	Pulse Repetition Frequency
RA	Radar altimeter
RADAR	Radio Detection and Ranging
RTM	Radiative Transfer Model
SAR	Synthetic Aperture Radar
SIC	Sea Ice Concentration
SIRAL	SAR/Interferometric Radar Altimeter
SIT	Sea Ice Thickness
SH	Southern hemisphere
SMMR	Scanning Multichannel Microwave Radiometer
SMOS	Soil Moisture and Ocean Salinity
SSM/I	Special Sensor Microwave / Imager
SSMIS	Special Sensor Microwave / Imager+Sounder
TB	Brightness Temperature
TBD	To be defined
TM	Thematic Mapper
UB	University of Bremen
UH	University of Hamburg
ULS	Upward Looking Sonar
URD	User Requirements Document
URL	Uniform Resource Locator
V	Vertical polarization

Table 1-3: Acronyms

2   Round Robin Data Package (RRDP) (Sea Ice Concentration)

The purpose of the RRDP is to collect a reference dataset of brightness temperatures (TBs) and validated sea ice concentrations as well as relevant auxiliary information that allow evaluation of sea ice concentration algorithms and understanding of the error contributions from different sources of errors.

The database consists of TB data measured by:

- AMSR-2

- AMSR-E,

The format of the RRDP is a set of data files in simple ASCII comma separated format with a number of columns containing:

- Reference ice/snow data (time, position, source, reference data, including total ice concentration, snow parameters (if known), ice type, ice thickness etc. if available);

- Associated environmental parameters (atmosphere from ECMWF reanalysis closest 3h forecast (DARD: ID 2.01)). *http://old.ecmwf.int/publications/manuals/d/gribapi/param/filter=grib1/order=paramId/order_type=asc/p=1/table=128/*

- AMSR-E and AMSR2 brightness temperature data (time, sensor, dataset-ID, TBs);

- ASCAT scatterometer data from IFREMER CERSAT (converted to 40 degree incidence angle by IFREMER)

- SMOS TB data (H and V) at 40 degree incidence angle from UH

- SMAP TB data at 40 degree incidence angle from UH

- QuikSCAT HH and VV backscatter data from IFREMER CERSAT

A number of reference data have been used

- Data from CRREL Ice Mass Balance Buoys *http://imb.erdc.dren.mil/buoysum.htm, Perovich, D., J. Richter-Menge, B. Elder, T. Arbetter, K. Claffey, and C. Polashenski, Observing and understanding climate change: Monitoring the mass balance, motion, and thickness of Arctic sea ice, http://imb.erdc.dren.mil , 2013.*

- Snow/Ice data from NASA's Operation Ice Bridge (OIB)

- Backtracked trajectories of 50 km segments from operation Ice Bridge using OSISAF ice drift data

- High latitude areas of no ice (identified using ice charts) (SIC0)

- High latitude areas of high ice concentration (~100%) identified from convergence in Winter SAR ice drift data. (SIC1)

- MODIS melt pond fraction and ice concentration data from University of Hamburg (UH)

- MERIS melt pond fraction dataset from University of Bremen (UB)

- SMOS thin ice thickness dataset from University of Bremen (thin ice areas identified in ENVISAT ASAR data)

- ICESAT Antarctic sea ice freeboard data preprocessed by ITU (Istanbul Technical University)

- ASPeCt ship observations of Antarctic sea ice and snow thickness and concentration (Worby et al), preprocessed by ITU

3   Reference data from SAR, VIS/IR, IMB, ICESAT, SMOS and OIB

For validation and process studies a Round Robin Data Package (aka a "match-up data base") has been created following the specifications given in the validation protocol. The RRDP is hereby made available for users in the sea ice and passive microwave science community. The RRDP consists of data based on:

- Data from areas of ~100% ice from quantification of convergence areas in ENVISAT ASAR, RADARSAT and Sentinel-1 ice drift data (DTU/DMI). Use convergence from ASAR/Radarsat/Sentinel-1 ice drift from high concentration ice areas, central Arctic as detection of 100% ice. Note: Summer data included, but not necessarily 100% ice.

- Data from high latitude areas of 0% ice concentration identified from ice charts, climatology and classified satellite images such as SAR discrimination between water and ice

- High quality validation dataset of large areas of ca. 100% thin ice (areas in the order of 100x100km) with ice thickness estimated from SMOS data

- Dataset of daily melt-season melt-pond cover fraction derived from MERIS imagery (2010-05-01 to 2010-08-08) (75x75 km cloud free areas)

- Time series of data along CRREL IMB buoy trajectories with reference ice- and snow thickness data as well as temperature profiles in the ice/snow.

- Data along Operation Ice Bridge flight tracks with OIB reference ice thickness and snow thickness.

- Backtracked trajectory data using OIB data as end-points, and OSISAF ice drift data for the backtracking through the winter.

- Freeboard data from ICESat

All data are collocated with available ERA Interim data, AMSR-E or AMSR2 data (brightness temperatures), ASCAT data, SMOS and SMAP data and QuikSCAT data.

We have developed the necessary collocation processing system based on satellite effective fields of view.

3.1   Collocation methods (SIC)

We use resolution matched AMSR data where all channels have been resampled using Baccus-Gilbert resolution matching. The target resolution for AMSR data is that of the 6.9 GHz channels (using the resolution matched AMSR-E dataset from NSIDC (Ashcroft & Wentz, 2013) and for AMSR2 we use the L1R data from JAXA (Maeda et al). All microwave radiometer data are extracted from swath TB datasets with exact time specification. ASCAT and QuikSCAT data are provided in daily gridded format by IFREMER at a 25 kimometer grid and we use the

nearest grid cell. SMOS and SMAP data are provided in daily gridded form by University of Hamburg, and we use the closest grid cell to the reference data.

3.2   Methods for deriving independent reference data

3.2.1   ASAR convergence method (SIC=100%)

The main method for identifying areas of 100% ice is based on the PolarView / MyOcean /CMEMS ice drift dataset from ENVISAT ASAR, Radarsat2 and Sentinel-1. This dataset is processed to find areas of ~100x100 km² with convergence in the ice drift pattern on two consecutive 1-day periods. During winter this will correspond to areas of total ice cover (assuming that we start on day 1 with near 100% ice). Eventual openings will after 2 days of convergence be either frozen or removed due to ridging/rafting. Since the areas are of the order of 100 km x 100 km we subsequently find corresponding satellite microwave radiometer data at similar resolution (see section 2.2) at all channels and where the resulting resolution cell is completely inside the 100x100 km² convergence area.

In the following, the method derived and the methods used for the identification of nominal 100% sea ice is described in more detail.

It should be noticed that this method only provides reliable 100% data in winter, so the summer data should be used with care, since biases may exist. In Summer remaining openings may not freeze over during the 2 days.

3.2.1.1   AOI (Area Of Interest) cell grid description

The extent of the geographical areas of interest covers for the northern hemisphere 55N to 90N, and for the southern hemisphere 55S to 80S as only sea ice is relevant.

To facilitate the identification of nominal 100% ice a special AOI grid has been devised.

The sea-ice covered areas are divided into round AOI grid cells each with a diameter of 100km and evenly spaced with approximately 50% overlap and at least 50km from land. The 50km distance is chosen to ensure that the antenna footprint of any available passive microwave measurement sample with a centre position inside an AOI cell does not cover any land.

3.2.1.2   Identification of nominal 100%

To identify locations with nominal 100% ice cover, the transport of ice is examined directly in the form of the DTU CMEMS SAR based sea ice drift product.

It is assumed that an observed area which conforms to specific set of criteria with respect to area changes indicates very near 100% ice cover. An observed ice-area must decrease slightly from day to day, as area

increase indicates lead formation and large decreases indicate too little ice. A basic assumption is that during winter, eventual openings in the ice on day 1 will either close due to the convergence or refreeze due to the cold weather. During Summer the latter part of this assumption does not hold, so the Summer data cannot be assumed to always represent close to 100% ice and should be used with caution.

Furthermore the observations must cover the AOI cell well.

The specific requirements set up is as follows

3.2.1.3 Compression zone identification

All drift observations for a given day are ordered in groups of 4 neighbours and the area change calculated using a free 3rd party tool called Planimeter available from http://geographiclib.sourceforge.net/ in the package GeographicLib.

The area-change observations from a period of nominally 24 hours are then sorted into the AOI 100 km grid, so that one AOI cell keeps track of all available area change observations that fall within its boundaries.

During this process the area observations are flagged at either 'good' or 'bad' depending on their characteristics.

For a single deformation observation to be considered 'good' the area change must lie within certain limits, these have been loosely chosen to be 95%-102% (slightly above 100% is accepted since the area change observations are noisy due to the round-off uncertainty associated with the 300 m resolution of the SAR data on which the sea ice drift product is based).

Following this only AOIs where the average area change of all observations are between 98 and 100% (0.98 and 1.00) are accepted. For an AOI cell full of observations to enter the RRDP, it must contain 40 or more 'good' cells.

3.2.2 High latitude open ocean (no ice) (SIC=0%)

From ice-charts we identify the limit of all ice and select areas in the order of 100 km away from the ice edge in the open water region. These areas provide the open water test data, and collocation with AMSR data is done in the same manner as above for the 100% ice areas.

The dataset contains 1 datapoint per day at each of these locations.

Table 2.1 Location and valid period for open water data points

| Northern hemisphere		Southern hemisphere	
January and February	**August and September**	**January, February, March, April**	**August, September, October, November**
58N 52W	65N 56W	64S 80W	60S 80W
63.5N 35W	63.5N 35W	63S 170W	58S 170W
70N 0E	70N 0E	59S 90E	55S 90E
73N 30E	75N 40E	64S 10E	50S 10W
55N 180	70N 170W	58.5S 20W	
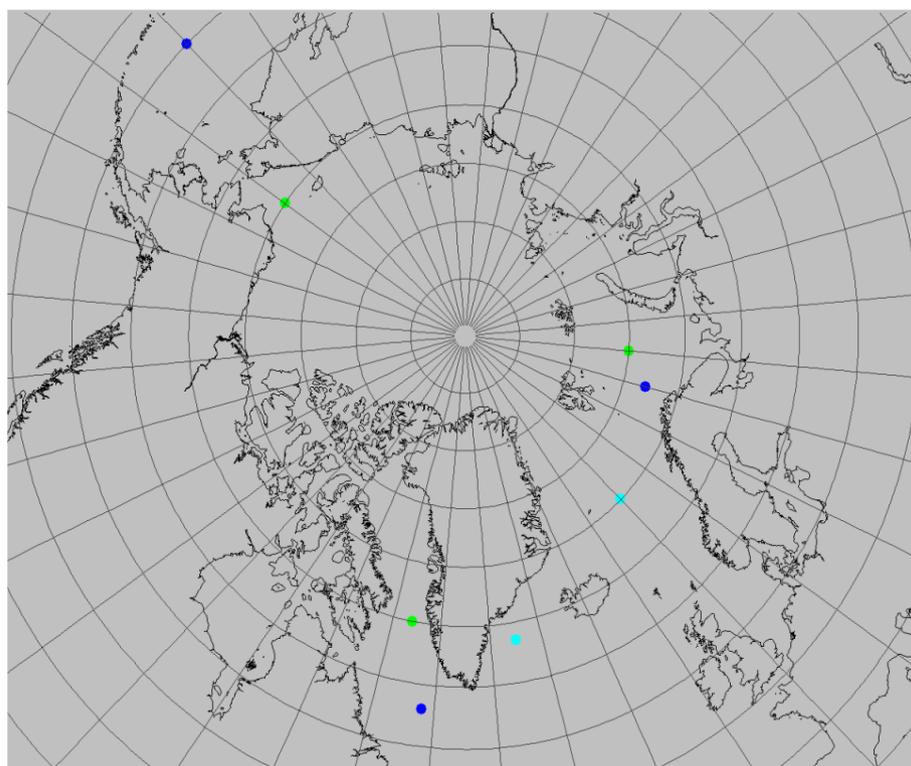
Figure 1. Location of areas for SIC=0 validation. Green are summer points, blue are winter points and cyan are points used all year.
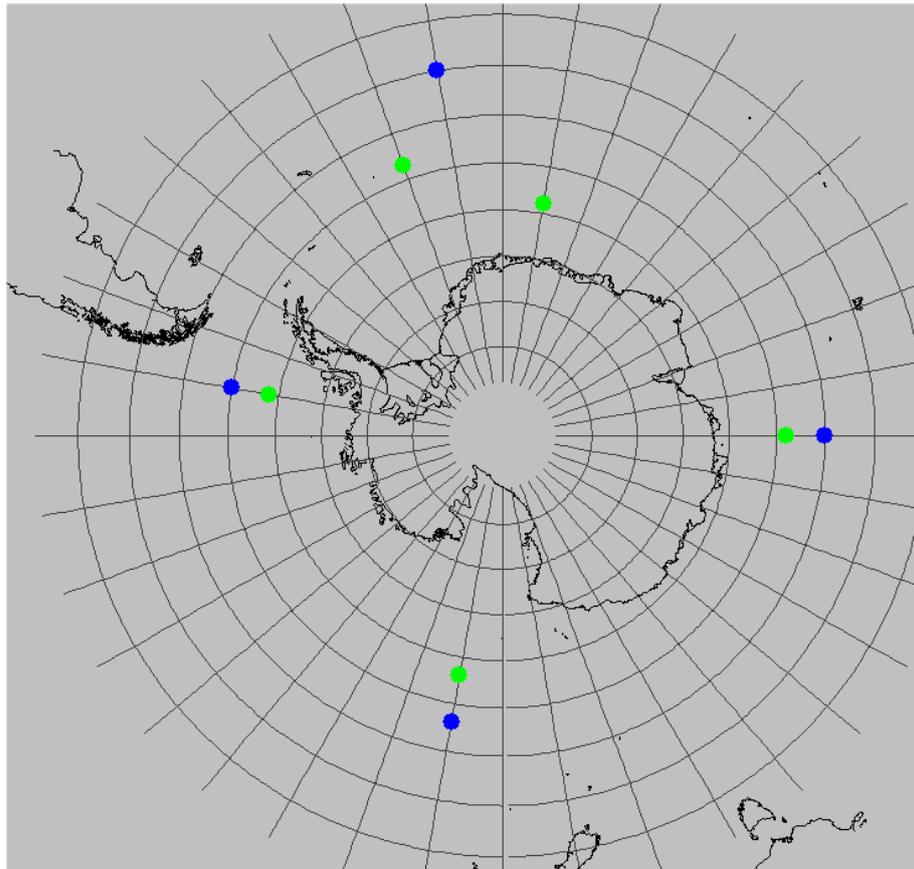
Figure 2. Location of SIC=0 areas for the Southern Hemisphere. Green are Austral Summer locations and blue are Austral Winter locations.

3.2.3   Thin ice thickness

Initially, regions of homogeneous thin sea ice have been visually identified using ENVISAT ASAR data. Large areas (~50 km radius) of fairly homogenous high concentration low backscatter ice is identified in the SAR data and date and center locations are recorded for subsequent SMOS ice thickness co-location.

ESA's L-band microwave radiometer sensor SMOS is intended to observe soil moisture and ocean salinity (name). Because of its long wavelength the observations are also suitable to retrieve the thickness of thin sea ice data (up to approximately 50 cm depending on salinity and temperature of the sea ice). Two algorithms have been suggested, one based on intensity and incidence angles below 40° (Kaleschke et al. 2012; Tian-Kunze et al., 2014), and one based on simultaneously using both intensity and polarization difference at incidence angles above 40° (Huntemann et al., 2014). Here, the latter procedure is applied to observations of the Arctic in the period of October to December 2010, the first Arctic freezing season which was observed by SMOS.

All processing is based on SMOS L1C version 3.46 data. These data are organized in Discrete Global Grid (DGG) cells of 9 km spacing in an

Icosahedral Snyder Equal Area projection with aperture 4 and resolution 9 (ISEA 4H9). The grid cells have a size of about 15x15 km². Observations closer than 50 km to land have been excluded. All SMOS snapshots containing one or more pixels with brightness temperature higher than 300 K are considered RFI contaminated and excluded.

Initially, regions of homogeneous thin sea ice have been visually identified using ENVISAT ASAR data. Large areas (~50 km radius) of fairly homogenous high concentration ice is identified in the SAR data and date and center locations are recorded for subsequent SMOS ice thickness co-location and co-location with AMSR TBs.

The mere SMOS ice thickness retrieval is organized in four steps:

1. convert observations of the four Stokes components from the instrument reference frame to the surface reference frame,
2. averaging of all observations of one day within one DGG and incidence angle range of 40° to 50°
3. retrieval of ice thickness based on intensity of polarization difference values
4. interpolate results to polar stereographic projection of 12.5 km (NSIDC grid).

The SMOS thin ice algorithm is developed for the Arctic so only northern hemisphere data is included.

3.2.4   Summer melt co-location

Gridded independent SIC and MPF estimates from MODIS (Rösel et al 2012)

Reflectances measured by bands 1, 3, and 4 of the MODIS sensor and provided by NASA as MODIS Surface Reflectance 8-Day L3 Global 500m SIN Grid V005" - product (MOD09A1) and "MODIS Surface Reflectance daily L2G Global 500 m and 1 km" - product (MOD09GA) are projected onto a polar-stereographic grid with 500 m grid resolution, applying land, cloud and other flags provided with the original MODIS product. The analysis is limited to tiles covering the Arctic Ocean, i.e. north of 60°N. A spectral un-mixing process is applied together with an artificial neural network to classify the reflectances of each grid cell into the three surface classes: open water, melt ponds, and snow / ice. For the final melt pond fraction product, surface class distributions are interpolated onto a 12.5 km grid resolution polar-stereographic grid; resulting netCDF files contain melt pond fraction (MPF), number of valid (non-flagged) 500 m grid cells per 12.5 km grid cell (N), standard deviation of MPF according to N (MPF-SD), and the open water fraction (OWF). This is the standard product which is available as 8-day composite via ICDC (http://icdc.zmaw.de) and which has been retrieved as 1-day product specifically for SICCI.

The RRDP requires high quality, high ice concentration data at 100 km grid resolution. For the RRDP product, a 100 km x 100 km grid product based on the average values of 8x8 12.5 km grid cells is computed for MPF, MPF-SD, and OWF. For this only those 12.5 km grid cells are used where the MODIS SIC, which is 100% minus OWF, is above 90% and where the cloud fraction is below 5%. It is further ensured that only grid

cells are used which are in at least 100 km distance to the coast. For the colocation of the 100km x 100km MPF product with PMW data all AMSR-E passes during the day are included (with a max distance to the center of the 100x100 km MODIS MPF grid cell area of 5 km).

3.2.5   MERIS Open Water fraction data from University of Bremen

These data are produced using the method described in (Istomina et al, 2015)

3.2.6   CRREL Ice Mass Balance Buoy (IMB) data

Time series of data along IMB buoy trajectories have been compiled. These data include snow/ice thickness and snow/ice temperature profile data. Data have been interpolated to every 6 hours in order to have continuous 6 hourly NWP accumulated fields. (Perovich et al 2017)
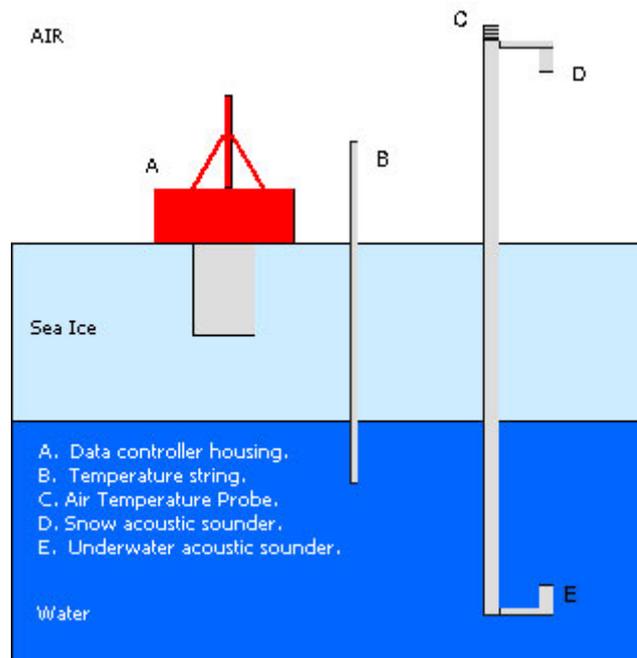
Figure. Sketch of installed buoy

The Ice Mass Balance Buoy (IMB) is an autonomous, ice-based system, designed to measure and attribute thermodynamic changes in the mass balance of the sea ice cover. The instrumentation of the autonomous mass balance buoys typically consists of a data controller module and Argos transmitter (image right, located inside A), a temperature string (B), above ice (D) and below ice (E) acoustic sounders measuring the positions of the snow/ice surface and ice bottom within 5 mm. In addition to the mass balance instrumentation the buoys have a barometer (mounted to A), and an air temperature sensor (C).

The current Thermistor strings made out of a PVC rod with thermistors mounted every 10 cm. These rods are easily connected to assemble strings that extended from the air through the snow and ice into the upper ocean. The thermistor accuracy is 0.1 C.

The data controller housing is typically a sealed 20 cm diameter aluminum tube. The controller housing contains the data controller. The data controller collects information from each instrument, processes and organizes the data, adds the date/time stamp and sends the data from the Buoy to our Laboratory. Currently, data transmissions are performed by the Iridium satellite phone communications system.

For measuring snow depth and top surface snow and ice ablation, we use an above ice acoustic sounder (rangefinder) made specifically for measuring snow depth. The sensor is mounted on a pole frozen into the ice, looking down at the snow surface. It measures distance between the instrument and the snow surface, thus recording the changes in the snow depth. When the snow melts in the summer, the instrument then measures surface ice ablation.

For the under ice acoustic sounder we use an underwater sonar altimeter mounted on a pole that is frozen into the ice and extends into the ocean. The sounder is installed so that it looks up at the underside of the ice sheet. It measures distance between the instrument and the ice bottom, thus recording the ice bottom growth and ablation.

Sea level pressure is measured using an electronic barometer. The barometer is usually mounted on the controller housing near the transmitter antennae.

The IMB Buoys are typically co-located with comlementary buoy packages put into place by our scientific partners. These packages have included web cameras looking at our installed IMB buoy and provide infromatoin on the areas ice surface morphology including melt pond coverage.   Links to co-located instrumentation packages are located on the individual IMB Buoy web pages.

3.2.7   Operation Ice Bridge (OIB) data

Since 2009 NASA's Operation Ice Bridge has collected ice and snow thickness data in the Arctic during annual flight campaigns (March-May). The data are especially valuable in this context since they contain snow thickness information from the snow radar. Original OIB data are averaged into 50 Km sections for better overlap/co-location with AMSR TB data. (Kurtz et al, 2013).
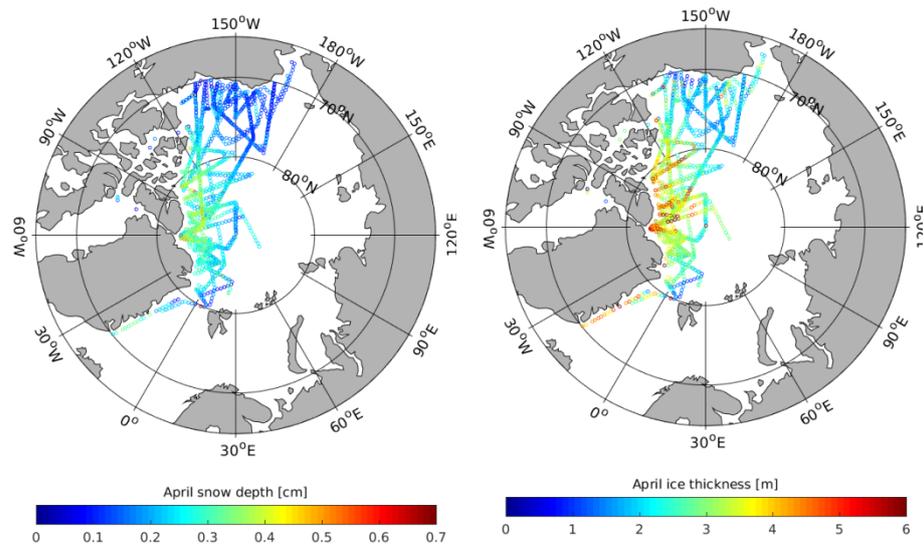
Figure. Operation Ice Bridge snow depth and ice thickness data (All OIB flight lines 2009-2015 (incl.)).

3.2.8   Backtracked Operation ice Bridge (OIB) data

A special extension to the direct operation ice bridge data is a set of backtracked OIB 50 km segments. The backtracking is performed using daily OSISAF ice drift data.

3.2.9   ICESat data (prepared by Istanbul Technical University (ITU))

This dataset contains average and standard deviations of freeboard measured by the ICESat satellite over the Southern Ocean.

3.2.10   ASPeCt and other in-situ Antarctic sea ice data (prepared by ITU)

This dataset contains various reference data from Antarctic Buoys and ASPeCT projects collocated with satellite data

4   Data sources and versions

4.1.1   ERA Interim data source and version

http://apps.ecmwf.int/datasets/data/interim-full-daily/levtype=sfc/

http://old.ecmwf.int/publications/manuals/d/gribapi/param/filter=grib1
/order=paramId/order_type=asc/p=1/table=128/

For more details see (Dee et al, 2011)

4.1.2   AMSR-E data source and version

The AMSR-E Level-2A product (AE_L2A) contains brightness temperatures available at a variety of resolutions that correspond to the footprint sizes of the observations. Each swath is packaged with associated geolocation fields.

The AMSR-E Level-2A product (AE_L2A) contains brightness temperatures at 6.9 GHz, 10.7 GHz, 18.7 GHz, 23.8 GHz, 36.5 GHz, and 89.0 GHz. Data are resampled to be spatially consistent, and therefore are available at a variety of resolutions that correspond to the footprint sizes of the observations such as 56 km, 38 km, 24 km, 21 km, 12 km, and 5.4 km, respectively. Each swath is packaged with associated geolocation fields. Data are stored in Hierarchical Data Format - Earth Observing System (HDF-EOS) format and are available from 19 June 2002 to the present via FTP.

Ashcroft, P. and F. J. Wentz. 2013. *AMSR-E/Aqua L2A Global Swath Spatially-Resampled Brightness Temperatures, Version 3*. [Indicate subset used]. Boulder, Colorado USA. NASA National Snow and Ice Data Center Distributed Active Archive Center. doi: http://dx.doi.org/10.5067/AMSR-E/AE_L2A.003.

http://nsidc.org/data/AE_L2A/versions/3

4.1.3   AMSR-2 data source and version

L1R AMSR-2 data from JAXA:

AMSR2 geophysical parameters are calculated by combining multiple AMSR2 frequencies and polarizations. In that case, there is no consistency with latitude and longitude of same observation point because of different footprint size. AMSR2 provides product call L1R that resamples the L1B product using pre-calculated resampling coefficients to adjust data for lower frequency resolutions (Maeda et al, 2012).

The center latitude and longitude of data is adjusted to the 89 GHz A channel receiver data.

Resampling converts the brightness temperature at a higher resolution frequency to a brightness temperature at a lower resolution frequency. Resampling data based on 6.9, 10.7, 23.8, 36.5GHz footprint size is created. 6 GHz and 7 GHz data sets have the same spatial resolution;

therefore, a shared set of resampling data is created. 18 GHz and 23 GHz data sets have almost the same resolution, but 23 GHz resolution is slightly lower; therefore, one set of resampling data is created matching the 23 GHz resolution. Table 6 shows L1R data and frequencies selected for resampling.

Table 6. L1R data and frequencies selected for resampling

Footprint	6G (H/V) 243 points	7G (H/V) 243 points	10G (H/V) 243 points	18G (H/V) 243 points	23G (H/V) 243 points	36G (H/V) 243 points	89G (H/V) 243 points	89G A-horn (H/V) 486 points	89G B-horn (H/V) 486 points
6GHz	☆	○	○	○	○	○	○		
10GHz			☆	○	○	○	○		
23GHz				○	☆	○	○		
36GHz						☆	○		
89GHz								△	△

○ indicate resampling data undergo spatial resolution conversion and processing for center latitude and longitude alignment.
☆ indicate resampling data only undergo processing for center latitude and longitude alignment.
△ indicate original observational data (same as L1B).
* 18 GHz and 23 GHz data sets have almost the same resolution, but 23 GHz resolution is slightly lower; therefore, one set of resampling data is created matching the 23 GHz resolution.

L1R stores resampling data of 6, 10, 23, 36GHz resolution, and original 89GHz data. L1R data marked by ☆ in Table 6 does not coincident with L1B data of same frequencies and polarizations, because processing for center latitude and longitude alignment is applied.

4.1.4   OIB data source and version

The NASA Operation IceBridge Mission, initiated in 2009, collects airborne remote sensing measurements to bridge the gap between NASA's Ice, Cloud and Land Elevation Satellite (ICESat) mission and the upcoming ICESat-2 mission.

IceBridge mission observations and measurements include coastal Greenland, coastal Antarctica, the Antarctic Peninsula, interior Antarctica, the southeast Alaskan glaciers, and Antarctic and Arctic sea ice.

The NASA IceBridge mission combines multiple instruments to map ice surface topography, bedrock topography beneath the ice sheets, grounding line position, ice and snow thickness, and sea ice distribution and freeboard. Data from laser altimeters and radar sounders are paired with gravitometer, magnetometer, mapping camera, and other data to provide dynamic, high-value, repeat measurements of rapidly-changing portions of land and sea ice.

We use data from the repository at NSIDC

4.1.5   CRREL IMB data source and version

http://imb.erdc.dren.mil/buoysum.htm

We include data from the upper 15 temperature sensors (spaced every 10 cm). We do not know the position of the sensors relative to the snow surface or snow/ice interface so users of the data requiring this information will have to extract it themselves by looking/processing the temperature profiles. An example of how this can be done is shown in the figure below.
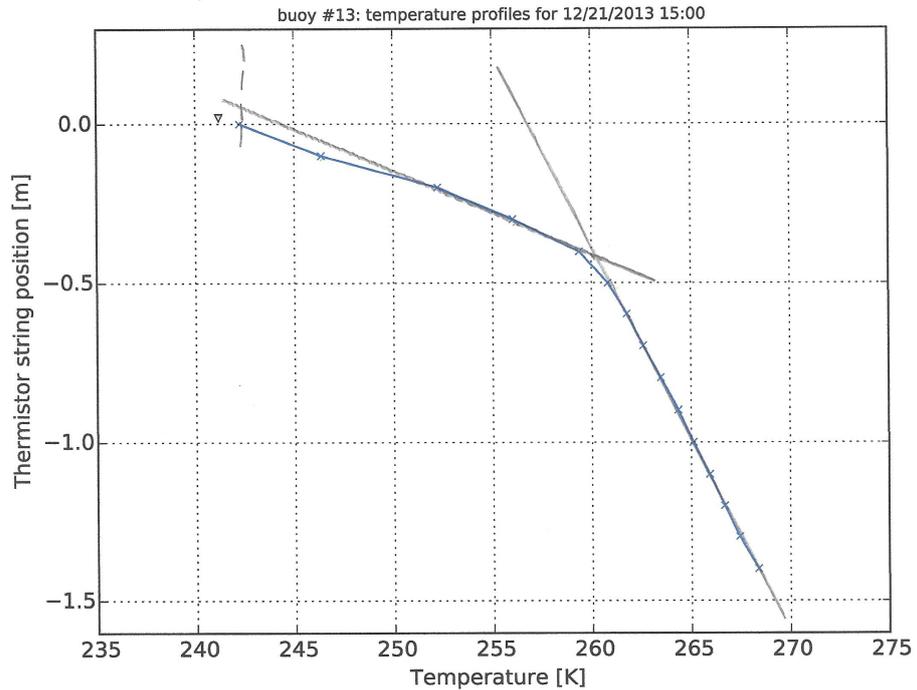
Figure: Construction of snow/ice interface and snow temperature gradient from CRREL IMB data with 10 cm temperature sampling.

4.1.6   MODIS MPF data source and version

The MODIS MPF data are produced by University of Hamburg using an algorithm developed by Rösel et al (2012). A special 1-day melt pond fraction dataset was produced for the RRDP.

Some comments to the MPF file in the RRDP:

1. Data with cloud fraction larger than 5% should NOT be used

2. MPF is a fraction of SIC, NOT of grid cell area

3. Data with SIC<95% should NOT be used

4. The MODIS SIC is all sea ice (including melt ponds).

So in order to get ISF (Ice Surface Fraction) which is the fraction of grid cell area that has ice at the surface (not melt ponds and not leads/open water), you should use

ISF=SIC-SIC*MPF or

ISF=SIC*(1-MPF)

4.1.7   **MERIS MPF data source and version**

Data provided by Larysa Istomina covers the period May to August 2011. The method cannot distinguish open leads from melt ponds, so the melt pond fraction may contain some lead fraction as well. However the data are predominantly from near 100% ice areas.

4.1.8   **ASCAT backscatter data**

ASCAT is a real aperture radar, operating at 5.255 GHz (C-band) and using vertically polarised antennas. It transmits a long pulse with Linear Frequency Modulation ('chirp').

Ground echoes are received by the instrument and, after de-chirping, the backscattered signal is spectrally analysed and detected. In the power spectrum, frequency can be mapped into slant range, provided the chirp rate and the Doppler frequency are known. The processing is, in effect, a pulse compression, which provides range resolution.

From around 837 km altitude, the instrument transmits well characterised pulses of microwave energy towards the sea surface. Winds over the sea cause small scale (centimetric) disturbances of the sea surface which modify its radar backscattering characteristics in a particular way.

These backscattering properties are well known and are dependent on both the wind speed over the sea and the direction of the wind, with respect to the point from which the sea surface is observed.

On board ASCAT, two sets of three antennas measure the resultant electromagnetic backscatter from the wind-roughened ocean surface, in two 500 km wide swaths, on each side of the satellite ground track. The three antennas on each side are oriented to broadside and ± 45° of broadside, and, so, make sequential observations of the backscattering coefficient of each point of interest from three directions. The three directions are needed to resolve the wind direction ambiguity.
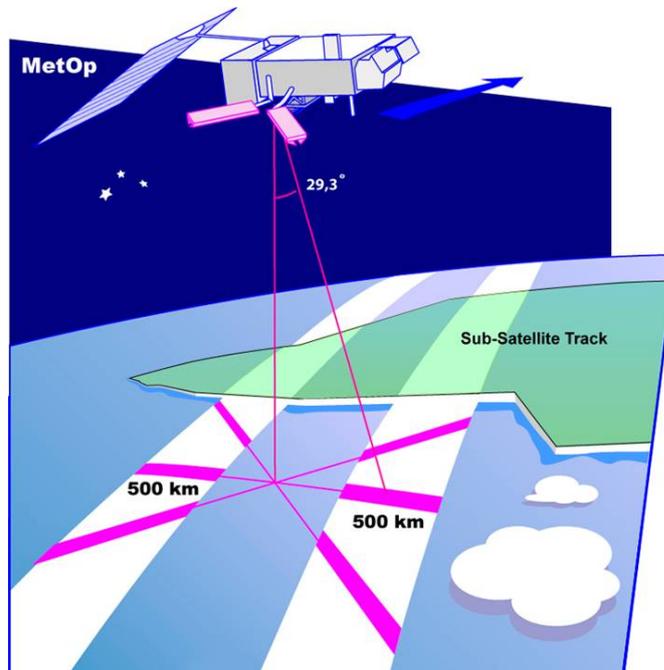

Figure 1. Graphic showing the field of vision of ASCAT

4.1.8.1   ASCAT Processing at IFREMER

Based on the experience from ERS and NSCAT data, IFREMER has developed algorithms to build incidence-adjusted backscatter maps. Fig.

2b shows incidence-adjusted backscatter map starting from the "raw" backscattered data presented in Fig. 2a. The incidence is 40°, as previously defined for fan-beam scatterometer.

This value is in the middle of the incidence range of ASCAT.

Signatures of swaths are corrected in Fig. 2b in comparison with Fig. 2a, and backscatter values have homogeneous geophysical meaning : high values at the North of Canada correspond to thick and multi-year ice (rough surface), and low values at the North of Russia to first-year ice (smooth surface). Geophysical structures are clearly detected

For more information see references by Ezraty et al.
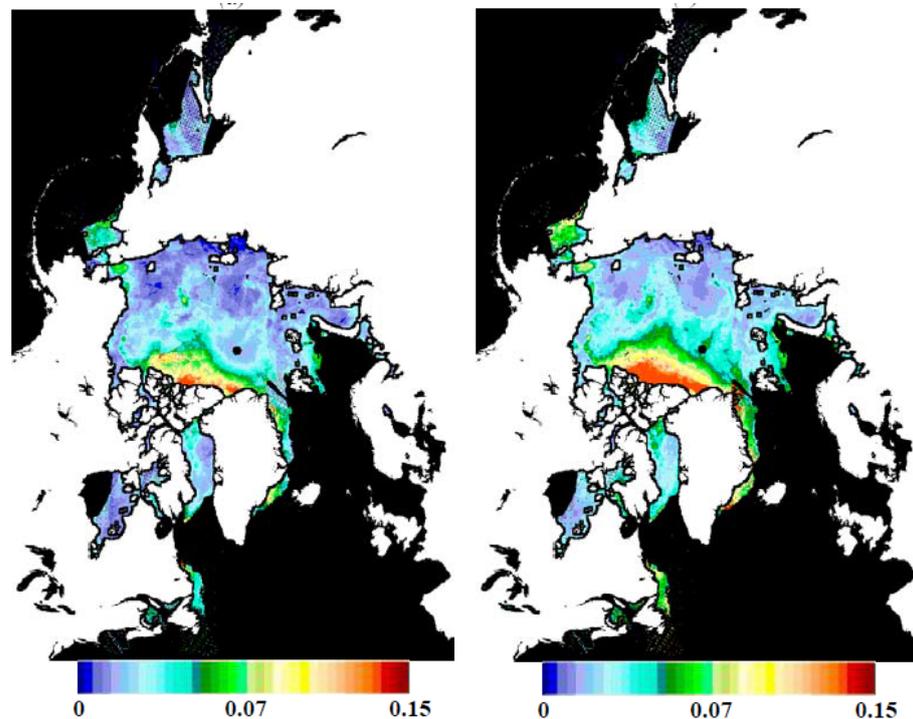
Figure 2. ASCAT backscatter maps from February 18, 2007. Left: ASCAT raw data. Right: ASCAT incidence-adjusted backscatter map at 40 degree incidence angle.

4.1.9 SMOS TB data (University of Hamburg)

The data used for the gridded SMOS TB product are based on the SMOS L1C brightness temperature data in version v620. The L1C product contains polarized multi-incidence angle TBs at the top of the ionosphere (TOI) geolocated in an ISEA grid with a grid size of 15 km. We apply a Faraday rotation correction using the given Faraday rotation angles to calculate TBs at the top of the atmosphere (TOA).

To obtain TBs at the SMAP incidence angle of 40°, all measured TBs during one day are collected at each grid point and a two-step regression is applied to fit separate functions to the TB components (Zhao et al. 2015). A detailed description of the fitting procedure is given in deliverable D6.4. The fitted TBs at 40° are then re-gridded to a polar EASE-grid 2.0 with a grid size of 12.5 km.

The uncertainty of the daily TB values is estimated from the root mean squared error (RMSE) of the measured values and the fitted curves.

4.1.10   **SMAP TB data (University of Hamburg)**

The data used for the gridded SMOS TB product are based on the SMAP L1B TB brightness temperature data in version 3 (Piepmeier et al. 2016). The L1B product contains swath data of time-ordered geolocated brightness temperatures as well as various correction terms (e.g. for extra-terrestrial radiation sources and atmospheric effects). To get a matching dataset to the SMOS TOA TBs we produce SMAP TBs at the top of the atmosphere that are only corrected for Faraday rotation and not for other radiation sources that impact the measured brightness temperatures.

All polarized TB values of one day are collected and gridded to a polar EASE-grid 2.0 with a grid size of 12.5 km using an inverse distance weighting gridding scheme with a search radius of 25 km (for details see deliverable D6.4).

A widely used method to estimate the uncertainty of averaged data x_i is the standard error, which is the sample standard deviation divided by the square root of the sample size n:

$$\frac{\sqrt{\frac{1}{n}\sum_{i=1}^{n}(x_i - \bar{x})^2}}{\sqrt{n}}.$$

For a weighted average, however, the calculation of the standard error is not trivial and there is no widely accepted definition. Therefore – as a rough estimate of the standard error – we divide the weighted sample standard deviation by an effective sample size n_{eff}. The effective sample size is estimated as the number of weights that cumulatively sum up to more than 80% of the total weights.
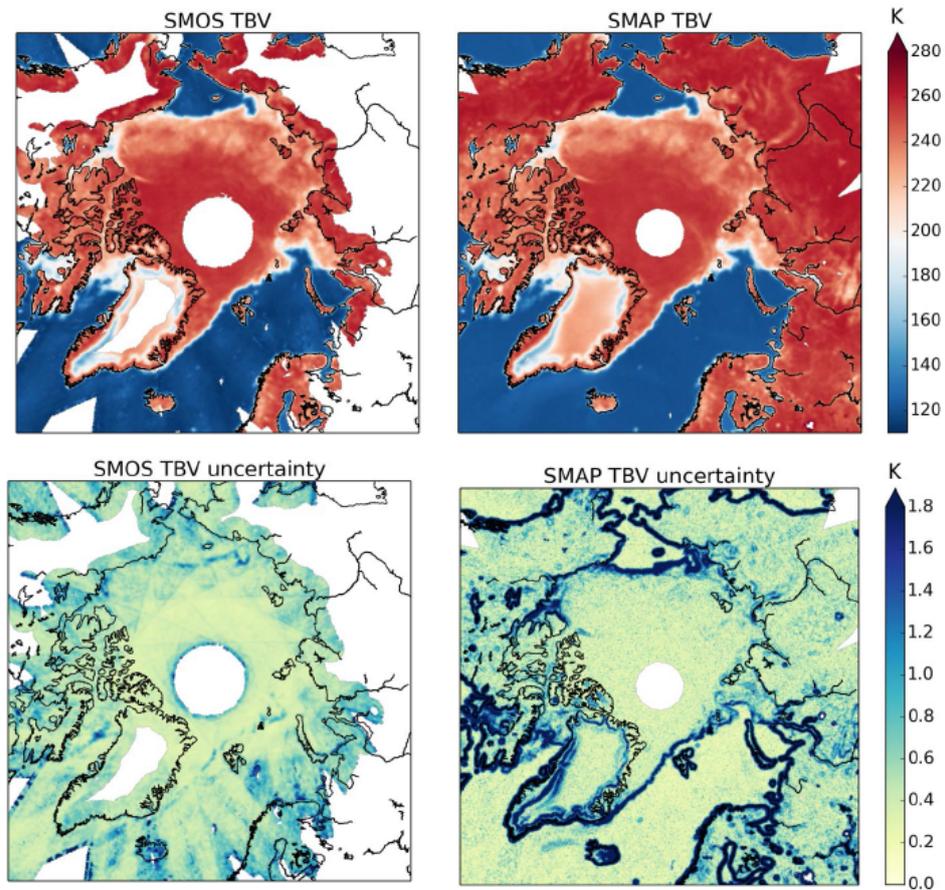
Figure. Brightness temperatures (upper) at vertical polarization from SMOS (left column) and SMAP (right column) and uncertainties (lower) on 5 November 2015.

4.1.11   QuikSCAT backscatter data source and version

Since winter 1999-2000, daily SeaWinds QuikSCAT Ku-band backscatter maps over the Arctic are regularly produced at IFREMER/CERSAT. Detailed description of this product, including validation of the sea ice/open ocean discrimination can be found in the user's manual (Ezraty and Piollé, 2001).

The projection used for these maps is that of the National Snow and Ice Data Center (NSIDC) with an almost constant grid size of 12.5 km x 12.5 km (see Section 1.2 in Ezraty et al., 2007a).

Time period: 19 July 1999 to 2009
Polarizations: V-Outer/H-inner
Frequency: 13.4 GHz (Ku band)
Resolution: 25 x 30 km (egg), 25 x 6 km (slice)
Swath width: 1400 km (inner (HH)) / 1800 km (outer (VV))

4.1.11.1   Construction of the QuikSCAT composite backscatter map

The figure below presents a sample of backscatter maps obtained from the inner (HH) and outer (VV) beams of SeaWinds, limited to the central Arctic

0 < inner beam (HH) < 0.250   *0 < outer beam (VV) < 0.208*
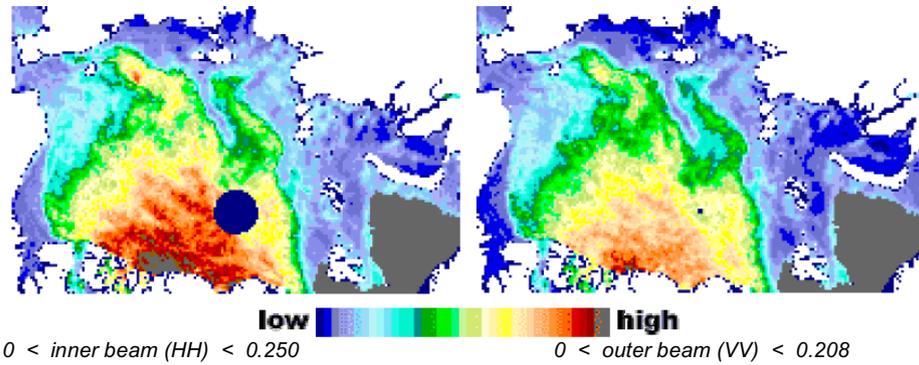
Figure: SeaWinds backscatter maps on February 23rd, 2002 (left: inner beam (HH), right: outer beam (VV))

At the North pole, because of the sensor geometry and the satellite orbits, areas of systematic missing data occur. The missing backscatter values of the inner beam at the North pole are estimated from the outer beam data using a third order polynomial fit; the coefficients of which are estimated from the 61 x 61 pixels surrounding this no-data area.
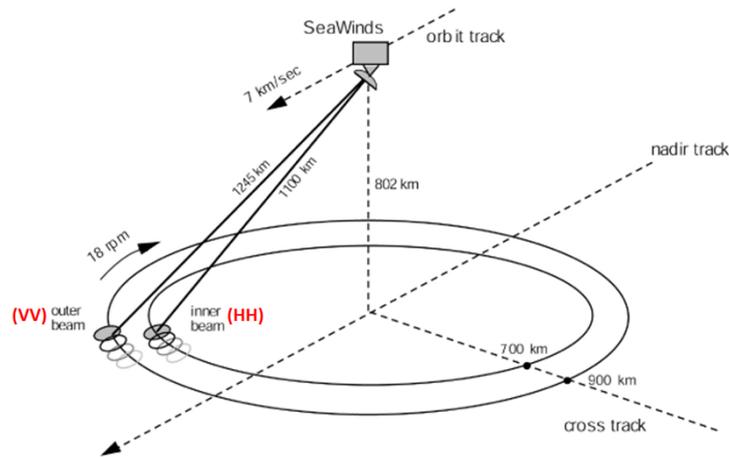
Figure: QuikSCAT viewing geometry (Image courtesy of Spencer, Wu, and Long (2000))

Data extend from 19 July 1999 to 31 December 2009. Table 1 lists the dates for which data are missing.

Table 1. Missing Dates

Year	Arctic Slices	Arctic Eggs	Antarctic Slices	Antarctic Eggs
2001	Days 132, 133, 189	Days 132, 133, 178, 189	Days 132, 133, 189	Days 132, 133, 175, 189
2002	N/A	N/A	Day 091	N/A
2005	N/A	N/A	Day 40	Day 55
2006	Day 197	Day 197	Day 197	Day 197
2008	Days 332, 333	Days 332, 333	Days 332, 333	Days 226, 332, 333
2009	Days 328 – 365	Days 328 – 365	Days 328 – 365	Days 328 – 365

QuikSCAT data. Periods with missing data (from NSIDC.
https://nsidc.org/data/docs/daac/nsidc0265_scatterometry_ice_extent.
gd.html).

5   SIC RRDP data format

We have produced a set of simple to use comma separated flat ASCII files. Each line records comma separated information for a unique (validation data, collocated satellite data) pair. The latitude, longitude, time, source/institution, reference SIC value are part of the information recorded.

Files consists of up to 7 sections

1. The reference data section (location, time, reference data). *This section varies between reference data types*

2. The NWP data section with data from ERA Interim

3. The AMSR data section with co-located AMSR data

4. The ASCAT data section with co-located ASCAT data

5. SMOS data section with co-located SMOS data

6. SMAP data section with co-located SMAP data

7. QuikSCAT data section with co-located QuikSCAT data

Finally a unique data identifier is added in the last column.

Below we present a detailed description of the data columns in each type of RRDP files.

The following sections describe the content of these datasections.

The reference data sections differ between types of reference data, whereas the satellite data sections and NWP sections are always the same.

5.1   100% SIC reference data section

The following tables contain information about the columns in each type of RRDP files.
Each line of each file contains a reference part and an observation part.
All values/IDs are separated by commas ","

Reference data section (SIC1)	
latitude	Reference latitude
longitude	Reference Longitude
time	Reference time
identification	Reference ID (COMPRESSIONCELLS_DTU)
SIC	Reference sea ice concentration (1)

5.2   0% SIC reference data section

Reference data section (SIC0)	
latitude	Reference latitude
longitude	Reference Longitude
time	Reference time
identification	Reference ID (ICECHART_DMI)
SIC	Reference sea ice concentration (0)

5.3   CRREL IMB reference data section

The following is a list of columns in the IMB reference datafiles

Reference data section (CRREL IMB)	
latitude	Reference latitude
longitude	Reference longitude
time	Buoy/reference time - Interpolated to 6h
identification	Buoy ID (e.g. BUOY_CRREL_2012B)
timedifference(sec)	Time difference (always 0)
Date	Buoy/reference time
Latitude (degrees)	Buoy latitude
Longitude (degrees)	Buoy longitude
Quality (+/- km)	Location quality (GPS)
Air Temp (C)	Air temperature ©
Air Pressure (mb)	Air pressure (mb)
Snow Surface Position (m)	Snow surface position (m)
Ice Thickness(m)	Ice thickness (m)
Ice Surface Position (m)	Ice surface position (m)
Ice Bottom Position(m)	Ice bottom position (m)
T1 (C)	Buoy IMB temperature (C)
T2 (C)	Buoy IMB temperature (C)
T3 (C)	Buoy IMB temperature (C)
T4 (C)	Buoy IMB temperature (C)
T5 (C)	Buoy IMB temperature (C)
T6 (C)	Buoy IMB temperature (C)
T7 (C)	Buoy IMB temperature (C)
T8 (C)	Buoy IMB temperature (C)
T9 (C)	Buoy IMB temperature (C)
T10 (C)	Buoy IMB temperature (C)
T11 (C)	Buoy IMB temperature (C)
T12 (C)	Buoy IMB temperature (C)
T13 (C)	Buoy IMB temperature (C)
T14 (C)	Buoy IMB temperature (C)
T15 (C)	Buoy IMB temperature (C)

5.4   Operation Ice Bridge (OIB) reference data section

The following table contains a list of the Operation Ice Bridge reference data columns.

Reference data section (OIB)	
latitude	Reference latitude
longitude	Reference Longitude
time	Reference time
identification	Reference ID (OIB_50KM_NERSC)
sd_mean	Snow depth average
sd_std	Snow depth st dev
sit_mean	Sea Ice Thickness average
sit_std	Sea Ice Thickness st dev
pcnt_ow_mean	% open water in 50 Km section
pcnt_ow_std	St dev of % open water in 50 Km section
pcnt_thin_ice_mean	% thin ice in 50 Km section
pcnt_thin_ice_std	St dev of % thin ice in 50 Km section
pcnt_grey_ice_mean	% grey ice in 50 Km section
pcnt_grey_ice_std	St dev of % grey ice in 50 Km section
surface_roughness_mean	Surface roughness (average over section)
surface_roughness_std	Surface roughness stdev over section
num_per_segment	Number of datapoints in 50 Km segment
delta_mean	
delta_gt_0_5	

5.5   MODIS Melt Pond Fraction reference data section

Reference data section (UH-MELT)	
latitude	Reference latitude
longitude	Reference Longitude
time	Reference time
reference-id	Reference ID (OIB_50KM_NERSC)
MPF[%]	MODIS melt pond fraction in 100 Km diameter area
MPF_STDDEV[%]	stdev of MODIS melt pond fraction in 100 Km diameter area
MPF_grid_cell_STDDEV[%]	
numcells	Number of used 12.5 Km cells
SIC[%]	Average MODIS Sea Ice Concentration (%) in 100 Km diameter area
SIC_grid_cell_STDDEV[%]	St dev of MODIS Sea Ice Concentration (500 m cells)
NUMCELLS	Number of used 12.5 Km
AVGnum_clear-sky_500m_pixels	Average number of clear sky 500m pixels
cloud_fraction_[%]	Cloud fraction (%)

5.6   MERIS melt pond fraction reference data section

Reference data section (UB-MELT)	
latitude	Reference latitude
longitude	Reference Longitude
time	Reference time
reference-id	Reference ID (MERISMELTPONDFRACTION_UB)
MPF (fraction of total area)	MERIS melt pond fraction in 100 Km diameter area (fraction of total area)
Stdev	stdev of MERIS melt pond fraction in 100 Km diameter area
Cloudmax	Maximum cloud cover (5% or 1%)

5.7   Thin ice thickness data reference data section

The following table lists the variables included in the reference section of the SMOS thin ice datafiles

Reference data section (UB-THIN)	
latitude	Reference latitude
longitude	Reference Longitude
date	Reference time (only date, since all data are from daily mosaics)
reference-id	Reference ID (THINICE_UB)
SIC	Nominal sea ice concentration (1.0)
SIT	SMOS thin ice thickness (m) (note that all datapoints with SIT>0.5m are given as 0.51m)

5.8   ICESat freeboard reference data section

The following table lists the variables included in the reference section of the ICESat freeboard datafiles

Reference data section (UB-THIN)	
latitude	Reference latitude
longitude	Reference Longitude
timestamp	Reference time (only date, since all data are from daily mosaics)
reference-id	Reference ID (ex. ITU_ICESAT_2008_3J)
50km_avg_FB	50 km average freeboard
50km_std_res_elv	50 km standard deviation of residual elevation

5.9 The NWP section

The following table lists the variables in the NWP section of each RRDP file (Dee et al, 2011)

ERA Interim section	# ERA: v20150911 noval gapfill
latitude	ERA Interim Latitude
longitude	ERA Interim Longitude
time	ERA Interim time
reference-id	NWP_ECMWF
upstreamfile	Name of ERA Interim file (Internal)
msl	Mean sea level pressure (hPa)
u10	Wind speed 10 m (u component) (m/s)
v10	Wind speed 10 m (v component) (m/s)
ws	Wind speed (m/s)
t2m	2 m air temperature (K)
skt	Skin temperature (K)
istl1	Ice temperature layer 1 (0-7 cm)
istl2	Ice temperature layer 2 (7-28 cm)
istl3	Ice temperature layer 3 (28-100 cm)
istl4	Ice temperature layer 4 (100-150 cm)
sst	Sea surface temperature
d2m	2 m dew point temperature
tcwv	Total columnar water vapour (kg/m2)
tclw	Total columnar liquid water (kg/m2)
tciw	Total columnar ice water (kg/m2)
ssrd	Surface solar radiation downwards (W/m2) (average of accumulated radiation over the previous 6h)
strd	Surface thermal radiation downwards (W/m2) (average of accumulated radiation over the previous 6h)
e	Evaporation (m of water equivalent) (Accumulated previous 6h)
tp	Total precipitation (m) (Accumulated previous 6h)
sf	Snow fall (m of water equivalent) (accumulated previous 6h)
fal	Forecast albedo (0-1)
ci	ERA Interim Ice Concentration

Note that in versions before 2.2 the ssrd and strd was erroneously stated to be J/m2. However, the values given were (and are) the accumulated radiation over 6h divided by the number of seconds in 6h (21600 s). To get the original ERA-Interim accumulated radiation in J/m2, you should multiply our values by 21600 s.

Note also that the accumulated radiation over 6 h is only correct (and relevant) in the time series files (CRREL-IMB and OIB-backtrack). In all other files the accumulation was done erroneously. This error also pertains to accumulated variables of ERA-Interim in the CRREL-IMB and OIB-backtrack files before version 2.2.

5.10   The AMSR data section

This section is the same for AMSR-E and AMSR2 datafiles. In the ASMR-E files the 7.3GHz columns are filled with noval.

AMSR section	AMSRX: v201602 noval gapfill nearest 1.5h/5km + timediff parameter
latitude	AMSR Latitude
longitude	AMSR Longitude
time	AMSR time
identification	AMSR ID
6.9GHzH	AMSR channel TB (K)
6.9GHzV	AMSR channel TB (K)
7.3GHzH	AMSR channel TB (K) (noval for AMSR-E period)
7.3GHzV	AMSR channel TB (K) (noval for AMSR-E period)
10.7GHzH	AMSR channel TB (K)
10.7GHzV	AMSR channel TB (K)
18.7GHzH	AMSR channel TB (K)
18.7GHzV	AMSR channel TB (K)
23.8GHzH	AMSR channel TB (K)
23.8GHzV	AMSR channel TB (K)
36.5GHzH	AMSR channel TB (K)
36.5GHzV	AMSR channel TB (K)
89.0GHzH	AMSR channel TB (K)
89.0GHzV	AMSR channel TB (K)
Earth Incidence	Earth Incidence angle
Earth Azimuth	Earth azimuth angle
scanpos	Scanpos (0-243)
upstreamfile	Name of AMSR file
timediff	Time difference between reference time and AMSR time (seconds)

5.11   The ASCAT section

This section contains ASCAT data from IFREMER CERSAT

ASCAT section	ASCAT: v20160329 static grid fix
latitude	ASCAT latitude
longitude	ASCAT longitude
time	ASCAT time
reference-id	ASCAT_CERSAT_IFREMER
upstreamfile	Name of ASCAT file (ex. ASCAT_20140726.nc)
sigma_40	ASCAT backscatter (dB)
sigma_40_mask	ASCAT backscatter (dB) - masked
nb_samples	Number of ASCAT samples
warning	ASCAT flag
std	Standard deviation of ASCAT data

5.12   The SMOS section

This section contains SMOS data from University of Hamburg

SMOS section	SMOS
latitude	SMOS latitude
longitude	SMOS longitude
time	SMOS time
reference-id	SMOS_UHAM
upstreamfile	Name of SMOS data file (ex. SMOS_40deg_e12.5_20101118.nc)
SMOS_Tbv	SMOS TBV (at 40 deg incidence angle)
SMOS_Tbh	SMOS TBH (at 40 deg incidence angle)
SMOS_RMSE_v	Stdev of TBV
SMOS_RMSE_h	Stdev of TBH
SMOS_nmp	Number of data points in daily map
SMOS_dataloss	Number of invalid data points (potentially RFI contaminated)

5.13   The SMAP section

This section contains SMAP data from University of Hamburg

ASCAT section	ASCAT: v20160329 static grid fix
latitude	SMAP latitude
longitude	SMAP longitude
time	SMAP time
reference-id	SMAP_UHAM
upstreamfile	Name of SMOS data file (ex. SMAP_40deg_e12.5_20150402.nc)
SMAP_Tbv	SMAP TBV (at 40 deg incidence angle)
SMAP_Tbh	SMAP TBH (at 40 deg incidence angle)
SMAP_RMSE_v	Stdev of TBV
SMAP_RMSE_h	Stdev of TBH
SMAP_nmp	Number of datapoints in daily map

5.14   The QuikSCAT section

This section contains QuikSCAT data from IFREMER CERSAT

QuikSCAT section	QUIKSCAT: v20160329 static grid fix
latitude	QUIKSCAT latitude
longitude	QUIKSCAT longitude
time	QUIKSCAT time
reference-id	QSCAT_CERSAT_IFREMER
upstreamfile	Name of QUIKSCAT file (ex. 20090405-L3-PSI-NH-1D_012-QSCAT.nc)
sigma0_inner	QUIKSCAT backscatter (dB) (HH)
sigma0_mask_inner	QUIKSCAT backscatter (dB) – masked (HH)
nb_inner	Number of QUIKSCAT samples (HH)
std_inner	Standard deviation of nb_inner datapoints in daily map (HH) - (not dB)
sigma0_outer	QUIKSCAT backscatter (dB) (VV)
sigma0_mask_outer	QUIKSCAT backscatter (dB) – masked (VV)
nb_outer	Number of QUIKSCAT samples (VV)
std_outer	Standard deviation of nb_outer datapoints in daily map (VV) - (not dB)

5.15   The data identifier section

At the end of each dataline you find a unique data identifier.

Data identifier section	ID number unique to this RRDP version in last field
RRDP_ID	Unique data id

6   Access the RRDP datafiles

The RRDP files are accessible from

http://www.seaice.dk/ecv2/rrdb-v1.0/SICCI-RRDP-V1.0.zip

and from figshare.com

7   References

Ashcroft, P. and F. J. Wentz. 2013. *AMSR-E/Aqua L2A Global Swath Spatially-Resampled Brightness Temperatures*. Version 3. [indicate subset used]. Boulder, Colorado USA: NASA National Snow and Ice Data Center Distributed Active Archive Center. http://dx.doi.org/10.5067/AMSR-E/AE_L2A.003.

Dee, D. P., Uppala, S. M., Simmons, A. J., Berrisford, P., Poli, P., Kobayashi, S., Andrae, U., Balmaseda, M. A., Balsamo, G., Bauer, P., Bechtold, P., Beljaars, A. C. M., van de Berg, L., Bidlot, J., Bormann, N., Delsol, C., Dragani, R., Fuentes, M., Geer, A. J., Haimberger, L., Healy, S. B., Hersbach, H., Hólm, E. V., Isaksen, L., Kållberg, P., Köhler, M., Matricardi, M., McNally, A. P., Monge-Sanz, B. M., Morcrette, J.-J., Park, B.-K., Peubey, C., de Rosnay, P., Tavolato, C., Thépaut, J.-N. and Vitart, F. (2011), The ERA-Interim reanalysis: configuration and performance of the data assimilation system. Q.J.R. Meteorol. Soc., 137: 553–597. doi: 10.1002/qj.828

Ezraty R. and J. F. Piollé, 2001, *SeaWinds on QuikSCAT Polar Sea Ice Grids, User Manual*. CONVECTION report N°5, V1.1, August 2001. Greenland Sea Convection Mechanism and Their Implications, Fifth Framework Programme of the European Commission 1998 2002, Contract N° EVK2 2000 00058.

Ezraty R., F. Girard-Ardhuin and J. F. Piollé, 2007, *Sea ice drift in the Central Arctic estimated from SeaWinds/QuikSCAT backscatter maps*. User'sManual, Version 2.2,February2007b.
ftp://ftp.ifremer.fr/ifremer/cersat/products/gridded/psi-drift/documentation/quikscat.pdf

Heygster,G., M. Huntemann, H. Wang 2012: *Polarization-based SMOS sea ice thickness retrieval algorithm (Algorithm Theoretical Basis Document (ATBD)*). Technical Report, Institute of Environmental Physics, University of Bremen.

Istomina, L., Heygster, G., Huntemann, M., Schwarz, P., Birnbaum, G., Scharien, R., Polashenski, C., Perovich, D., Zege, E., Malinka, A., Prikhach, A., and Katsev, I.: Melt pond fraction and spectral sea ice albedo retrieval from MERIS data – Part 1: Validation against in situ, aerial, and ship cruise data, The Cryosphere, 9, 1551-1566, https://doi.org/10.5194/tc-9-1551-2015, 2015.

Kaleschke, L., X. Tian-Kunze, N. Maaß, M. Mäkynen, and M. Drusch, *Sea ice thickness retrieval from SMOS brightness temperatures during the Arctic   freeze-up period*, Geophys. Res. Lett., 39, L05501,   doi:10.1029/2012GL050916, 2012

Kurtz, N., S. Farrell, M. Studinger, et al. 2013. "Sea ice thickness, freeboard, and snow depth products from Operation IceBridge airborne data." The Cryosphere, 7 (4): 1035–1056 [10.5194/tc-7-1035-2013]

Maeda, T, Y. Taniguchi and K. Imaoka, "GCOM-W1 AMSR2 Level 1R Product: Dataset of Brightness Temperature Modified Using the Antenna Pattern Matching Technique," in IEEE Transactions on Geoscience and Remote Sensing, vol. 54, no. 2, pp. 770-782, Feb. 2016. doi: 10.1109/TGRS.2015.2465170

Mäkynen, M., S. Kern, A. Rösel, and L. T. Pedersen, 2014, *On the estimation of melt pond fraction on the Arctic sea ice with Envisat WSM images*, IEEE Trans. Geosci. Rem. Sens., 52(11), doi:10.1109/TGRS.2014.2311476, 2014.

Perovich, D.K., J.A. Richter-Menge, B. Elder, K. Claffey, and C. Polashenski, Observing and understanding climate change: Monitoring the mass balance, motion, and thickness of Arctic sea ice, http://imb-crrel-dartmouth.org/ , 2017.

Rösel, A., Kaleschke, L., and Birnbaum, G.: Melt ponds on Arctic sea ice determined from MODIS satellite data using an artificial neural network, The Cryosphere, 6, 431-446, https://doi.org/10.5194/tc-6-431-2012, 2012.

Spencer, M. W., C. Wu, and D. G. Long. 2000. *Improved Resolution Backscatter Measurements with the SeaWinds Pencil-beam Scatterometer*. IEEE Transactions on Geoscience and Remote Sensing 38(1): 89-104

Tetzlaff, A., L. Kaleschke, 2016, *D6.1 – Gridded product of SMOS and SMAP TB and uncertainties*, SPICES H2020 project deliverable, Hamburg, 2016

Worby, A. P., C. Geiger, M. J. Paget, M. van Woert, S. F Ackley, T. DeLiberty, (2008). *Thickness distribution of Antarctic sea ice*. J. Geophys. Res*., 113, C05S92, doi:10.1029/2007JC004254.

Appendix A   Format of input data

In order to speed up addition of new data to the RRDP, input reference data should be delivered to DTU in the form of comma separated text files with the following specification:

The first row of the file can contain eventual reference information (version number of the file etc). First character of the line should be #

The second row of the file should contain variable names separated by commas, and with no blanks in the variable names. Also this line should start with # as the first character.

The first 3 columns of the file should contain latitude, longitude and time.

Latitude and longitude as degrees and decimal degrees (NOT degrees, minutes etc).

Longitude should be given in the range [-180:180]

Time should be in the format YYYY-MM-DDThh:mm:ss

An example of an input file is shown in the figure below:

< End of Document >